

Catheter-Tissue Contact Optimizes Pulsed Electric Field Ablation with a Large Area Focal Catheter

Mary Clare Flaherty¹, Shephal Doshi², Jacob Laughner¹, Melinda Quan¹, and Ante Anic³

¹Galvanize Therapeutics Inc

²Pacific Heart Institute

³Klinicki bolnicki centar Split

November 17, 2023

Abstract

Introduction: Pulsed electric field (PEF) ablation relies on the intersection of a critical voltage gradient with tissue to cause cell death. Field-based lesion formation with PEF technologies may still depend on catheter-tissue contact (CTC). The purpose of this study was to assess the impact of CTC on PEF lesion formation with an investigational large area focal (LAF) catheter in a preclinical model. **Methods:** PEF ablation via a 10-spline LAF catheter was used to create discrete RV lesions and atrial lesion sets in 10 swine (8 acute, 2 chronic). Local impedance (LI) was used to assess CTC. Lesions were assigned to 3 cohorts using LI above baseline: No Tissue Contact (NTC: $[?][?]10\Omega$, close proximity to tissue), Low Tissue Contact (LTC: $[?]11-29\Omega$), and High Tissue Contact (HTC: $[?][?]30\Omega$). Acute animals were infused with triphenyl tetrazolium chloride (TTC) and sacrificed $[?]2$ hrs post-treatment. Chronic animals were remapped 30 days post-index procedure and stained with infused TTC. **Results:** Mean (\pm SD) RV treatment sizes between LTC (n=14) and HTC (n=17) lesions were not significantly different (depth: 5.65 ± 1.96 mm vs 5.68 ± 2.05 mm, $p=0.999$; width: 15.68 ± 5.22 mm vs 16.98 ± 4.45 mm, $p=0.737$) while mean treatment size for NTC lesions (n=6) was significantly smaller (1.67 ± 1.16 mm depth, 5.97 ± 4.48 mm width, $p<0.05$). For atrial lesion sets, acute and chronic conduction block were achieved with both LTC (N=7) and HTC (N=6), and NTC resulted in gaps. **Conclusions:** PEF ablation with a specialized LAF catheter in a swine model is dependent on CTC. LI as an indicator of CTC may aid in the creation of consistent transmural lesions in PEF ablation.

Catheter-Tissue Contact Optimizes Pulsed Electric Field Ablation with a Large Area Focal Catheter

Short Title: Optimizing PEF Ablation with Contact Detection

Shephal K Doshi, MD¹; Mary Clare Flaherty, BS²; Jacob Laughner, PhD²; Melinda Quan, BS²; Ante Anic, MD³

¹Pacific Heart Institute, Santa Monica, California, USA

²Galvanize Therapeutics, Redwood City, CA

³ Klinički Bolnički Centar (KBC) Split, Split, Croatia

Conflict of Interest Statement: Flaherty, Laughner, and Quan are paid employees of Galvanize Therapeutics. No other conflicts of interests exist.

Corresponding Author:

Name: Mary Clare Flaherty,

Address: 1325 Indiana St, Unit 102

San Francisco, CA 94107

Email Address: Mary.clare.flaherty@gmail.com

Abstract:

Introduction: Pulsed electric field (PEF) ablation relies on the intersection of a critical voltage gradient with tissue to cause cell death. Field-based lesion formation with PEF technologies may still depend on catheter-tissue contact (CTC). The purpose of this study was to assess the impact of CTC on PEF lesion formation with an investigational large area focal (LAF) catheter in a preclinical model.

Methods: PEF ablation via a 10-spline LAF catheter was used to create discrete RV lesions and atrial lesion sets in 10 swine (8 acute, 2 chronic). Local impedance (LI) was used to assess CTC. Lesions were assigned to 3 cohorts using LI above baseline: No Tissue Contact (NTC: $[?][?]10\Omega$, close proximity to tissue), Low Tissue Contact (LTC: $[?]11-29\Omega$), and High Tissue Contact (HTC: $[?][?]30\Omega$). Acute animals were infused with triphenyl tetrazolium chloride (TTC) and sacrificed $[?]2$ hrs post-treatment. Chronic animals were remapped 30 days post-index procedure and stained with infused TTC.

Results: Mean (\pm SD) RV treatment sizes between LTC (n=14) and HTC (n=17) lesions were not significantly different (depth: 5.65 ± 1.96 mm vs 5.68 ± 2.05 mm, $p=0.999$; width: 15.68 ± 5.22 mm vs 16.98 ± 4.45 mm, $p=0.737$) while mean treatment size for NTC lesions (n=6) was significantly smaller (1.67 ± 1.16 mm depth, 5.97 ± 4.48 mm width, $p<0.05$). For atrial lesion sets, acute and chronic conduction block were achieved with both LTC (N=7) and HTC (N=6), and NTC resulted in gaps.

Conclusions: PEF ablation with a specialized LAF catheter in a swine model is dependent on CTC. LI as an indicator of CTC may aid in the creation of consistent transmural lesions in PEF ablation.

Keywords: Arrhythmias, Pulsed Field Catheter Ablation, Local Impedance, Atrial Fibrillation, Local Impedance

Abbreviations:

- Catheter-Tissue Contact (CTC)
- Cryoablation (Cryo)
- Electroanatomic Mapping (EAM)
- Inferior Vena Cava (IVC)
- Interquartile range (IQR)
- Intracardiac Echocardiography (ICE)
- Local Impedance (LI)
- Hematoxylin & Eosin (H&E)
- Pulmonary Vein Isolation (PVI)
- Pulsed Electric Field (PEF)
- Radiofrequency (RF)
- Superior Vena Cava (SVC)
- Triphenyl Tetrazolium Chloride (TTC)

Funding: Galvanize Therapeutics sponsored and funded this study.

Introduction:

Pulmonary vein isolation (PVI) remains one of the most effective treatment strategies for atrial fibrillation¹. Thermal ablation technologies like radiofrequency (RF) and cryoablation (Cryo) rely on direct contact to effectively transfer energy to produce irreversible thermal damage to cardiac tissue and durable PVI²⁻⁴. After being introduced in oncology over 30 years ago^{5,6}, pulsed electric field (PEF) ablation has been developed as a primarily non-thermal modality for cardiac tissue ablation, achieved by applying short duration bursts of

high voltage electric fields. Cardiac myocytes within a critical voltage gradient area undergo cell death due to destabilization of the cell equilibrium⁷.

PEF ablation treatment size is dependent on several factors, including waveform characteristics, electrode configuration, and field interaction with target tissues⁷. Although it has been proposed that, unlike thermal modalities, PEF ablation may not be dependent on catheter-tissue contact (CTC) because of its field-based nature⁸, computational modeling data and *ex vivo* bench studies using a bipolar PEF system have demonstrated a profound treatment size dependence on catheter-tissue proximity⁹. Proximity and contact dependence for PEF ablation, however, has not been thoroughly examined *in vivo*.

We investigated the relationship between CTC and monopolar PEF ablation in a preclinical porcine model. This study sought to determine, 1) if CTC is necessary for effective PEF treatment, and 2) how CTC can be used to optimize PEF ablation workflows and efficacy.

Methods:

In ten animals, pre-ablation CTC between a novel large area focal (LAF) ablation catheter and cardiac targets was evaluated using a custom local impedance (LI) system, with guidelines established in previous pilot studies using intracardiac echocardiography (ICE), electrogram amplitude, and electroanatomic mapping (EAM). Isolated ventricular lesions and atrial lesion sets were created with varying amounts of CTC. Treatment size and isolation of targeted structures were examined at acute and chronic timepoints using EAM and histology.

Ablation System

An 8.5Fr, bi-directional, irrigated catheter (6mL/min) with a 10mm diameter spheroid tip comprised of 10 nitinol composite splines (**Figure 1A**) was connected to an investigational PEF system consisting of a generator and connection box (**Figure 1B**) (Galvanize Therapeutics; Redwood City, CA). The system is designed to create large focal lesions (**Figure 1C**) that reduce the number of applications required to create a typical lesion set. Monopolar PEF energy is delivered asynchronously using a proprietary biphasic waveform (25A, 1.6ms) that minimizes microbubble formation and muscle contraction. The system measures LI between each spline and a central ring electrode. LI information is displayed using a graphical representation of the catheter tip where a color and bar length changes represent increasing impedance on each spline (**Figure 1D**). The system is compatible with multiple EAM systems and is capable of creating electroanatomic maps of the heart and monitoring local electrograms (**Figure 1E**).

Preclinical Procedure

The study protocol was approved by the Institutional Animal Care and Use Committee of GMD Laboratories (Pomona, CA). Discrete ventricular lesions and atrial lesion sets were studied using a Yorkshire hybrid swine model (N=10, 50-70 kg, male and female) in acute (N=8) and chronic procedures (N=2). Chronic procedures included recovery post-index procedure and invasive remapping at 30 days to analyze lesion durability and pathology. All catheters were introduced via femoral access under inhaled anesthesia (isoflurane, 1-5%) and without paralytics. Intravenous heparin was administered to maintain an activated clotting time [?]³⁵⁰ seconds prior to catheter introduction.

Operators guided the LAF catheter into bloodpool to determine a no-contact location and establish a LI baseline. After navigating the catheter to the myocardium, electrograms and ICE were used to determine CTC. No catheter-tissue contact (NTC) with close proximity to tissue (approximately <2mm) induced [?]¹⁰Ω from baseline, Low catheter-tissue contact (LTC) induced [?]¹¹⁻²⁹Ω, and High catheter-tissue contact (HTC) induced [?]³⁰Ω (**Figure 2**).

Experimental Workflow

Ventricular Lesions

Ventricular lesions were created in the RV (4-6 applications/chamber) with lesions assigned to one of the 3

CTC cohorts prior to ablation. ICE and EAM were used to position lesions [?]20mm apart to prevent lesion overlap. Acute lesions were allowed to dwell for [?]2hrs prior to euthanasia to enable sufficient maturation¹⁰.

Atrial Lesion Sets

Lesion sets were created in the RA and LA in all animals. A posterior line was created from the superior vena cava (SVC) to the inferior vena cava (IVC) using 10mm center-to-center interlesion spacing. Similarly, PVI was performed around the inferior common pulmonary vein. Lesion sets were assigned to one of the 3 CTC cohorts prior to treatment. For LTC and HTC cohorts, all lesions were assigned LTC or HTC, respectively. For the NTC cohort (acute intercaval only), the beginning of an intercaval line was started with HTC, followed by 1-2 applications with NTC (using ICE to confirm close proximity to tissue and targeting LI response <10 Ω), and the remainder completed with HTC. EAM and pacing maneuvers were used to assess acute block across intercaval lines and isolation of pulmonary veins. In chronic animals, remapping was performed at 30 days to confirm durability of all lesion sets.

Gross Necropsy and Histology

Deeply sedated swine were perfused intravenously with 1% TTC, then euthanized with an intravenous bolus of 130-150mg/mL saturated potassium chloride. Hearts were explanted, examined, and photographed. Ventricular lesions were cross-sectioned and individually assessed and measured by a blinded operator using a digital microscope (Dino-Lite Edge, AnMo Electronics). Ventricular lesions and atrial lesion sets were formalin fixed and processed for histological evaluation with hematoxylin and eosin (H&E) and Masson's Trichrome stains.

Statistical Analysis

Eight samples (2s) of LI data from the spline with the highest delta from baseline were averaged to determine CTC before and after each ablation. Continuous variables are expressed as mean \pm standard deviation or median with interquartile range (IQR). Categorical variables are presented as counts or percentages. ANOVA was performed to determine significant between variable groups where appropriate, with p-values <0.05 considered significant. Statistical analyses were performed with Minitab (v21.1.1)

Results:

Ventricular Lesion Analysis

In 8 acute animals, 41 lesions were attempted using LI and ICE to guide the catheter to NTC (n=6), LTC (n=14), or HTC (n=17) with 37 of 41 lesions identified and cross-sectioned for analysis during necropsy. Four lesions were excluded because they could not be identified (n=1) or cross-sectioned (n=3). Starting impedance relative to bloodpool was [?]8 Ω (IQR, 7-9 Ω) for NTC, [?]19 Ω (IQR, 15-25 Ω) for LTC, and [?]42 Ω (IQR, 33-50 Ω) for HTC (**Figure 3A**). Comparison of pre-ablation impedance deltas confirmed all 3 groups were statistically distinct (HTC-LTC: p<0.005, HTC-NTC: p<0.005, LTC-NTC: p=0.006). No microbubbles, muscle contractions, induced arrhythmias, or ST-elevation were observed during index procedures. No endocardial trauma, thrombus, or char were observed acutely or chronically.

In 2 chronic animals, N=8 lesions were attempted (NTC: n=2, LTC: n=3, HTC: n=3). All LTC and HTC lesions were identified and cross-sectioned and no NTC lesions were identifiable after 30 days. Of the 6 identified lesions, 4 were transmural and therefore not measurable(**Supplemental Figure 1**). No adverse events were observed during the 30-day waiting period.

Representative acute lesions following TTC staining are provided for each cohort (**Figure 3B**). LTC and HTC lesions were similar in appearance and size (consistently >3mm depth), while NTC yielded superficial lesions, moderate endocardial blanching, or no visible effect. H&E and Masson's Trichrome (**Figure 1C**), revealed necrotic myocardium, mild edema, and early-stage fibrosis on ventricular lesions with no visible impact to surrounding vessels.

Figure 3C further represents the relationship between lesion size and CTC. Average RV lesion size was not significantly different between LTC and HTC cohorts (depth: 5.7 ± 2.0 mm vs 5.7 ± 2.1 mm, $p > 0.99$; width: 15.7 ± 5.2 mm vs 17.0 ± 4.5 mm, $p = 0.74$). Mean NTC lesion size was significantly smaller than mean LTC and HTC sizes (1.7 ± 1.2 mm depth, 6.0 ± 4.5 mm width, $p < 0.001$). Above a minimum threshold of $[?]10\Omega$, increasing CTC did not increase lesion depth. Lesion depth and width were not impacted by catheter orientation or spline placement once $[?]2$ splines reached $LI > [?]10\Omega$ (**Supplemental Figure 2**).

Atrial Lesion Set Analysis

Table 1 summarizes all atrial lesion sets by CTC cohort. LTC and HTC pre-ablation LIs were within the intended ranges for the attempted lesion sets. All LTC and HTC intercausal lines (Acute: LTC $n=3$, HTC $n=2$; Chronic: LTC $n=1$, HTC $n=1$) and PVIIs (Acute: $n=4$ LTC, $n=4$ HTC; Chronic: $n=1$ LTC, $n=1$ HTC) resulted in acute and chronic conduction block. NTC intercausal lines (HTC lesions interposed by 1-2 NTC lesions, Acute: $n=3$) resulted in visible gaps where NTC lesions were placed, and 0% conduction block.

Figure 4 displays representative acute and chronic maps and chronic histology for LTC and HTC intercausal lines. In both cohorts, the low-voltage area (< 0.1 mV) produced acutely corresponded to persistent low voltage and expansion of the low-voltage area after 30 days, reflected in gross pathological width measurements (LTC acute: 21.8 ± 4.5 mm vs chronic: 37.8 mm; HTC acute: 23.8 ± 3.4 mm vs chronic: 43.2 mm). No statistical difference was identified between acute LTC and HTC intercausal widths ($p = 0.62$). Histologically, sections showed similar morphological changes and tissue composition for LTC and HTC chronic atrial lesion sets. Acute atrial tissue showed necrotic cardiomyocytes, early-stage fibrosis, and sparing of blood vessels (**Figure 4, 1B & 2B**). Chronic histological sections revealed complete transmural lesions and clear distinction between healthy and ablated myocardium at the border zone (**Figure 4, 1D and 2D**) with complete fibrotic and fatty tissue replacement of the cardiomyocytes within the ablated region (**Figure 4, 1E and 2E**).

Figure 5 shows an example of the NTC intercausal line. Pre-ablation LI was significantly different between NTC and HTC regions ($[?]10 \pm 4$ vs $[?]35 \pm 8$, $p = 0.03$). The site of the NTC lesion shows a distinct unaffected high-voltage area ($[?]1$ mV) in comparison to the surrounding low-voltage ablated regions (< 0.1 mV) (**Figure 5A**). Gross pathology of all NTC intercausal lines revealed unaffected myocardium in the areas of NTC lesions (**Figure 5C**). Histological analysis revealed necrotic myocardium noted by contraction band necrosis, cell shrinkage, and irregular morphology on the transmural ablated HTC region (**Figure 5B**) versus healthy myocardium on the NTC region (**Figure 5D**).

Additional LI Analysis

There was no meaningful LI drop observed after PEF ablation for any cohort (NTC: 3Ω , LTC: 1Ω , HTC: 2Ω ; $p > 0.7$ for all cohort combinations). After 30 days, under guidance of EAM and ICE, the LAF catheter was placed in three areas of varying bipolar electrogram voltage: High-Voltage Zone ($[?]1$ mV), Border Zone (0.1 - 0.9 mV), and Scar Zone (< 0.1 mV). LI response was reduced in the border zone ($[?]12\Omega$, IQR: 10 - 14Ω) and scar zone ($[?]8\Omega$, IQR: 6 - 9Ω) compared to the high-voltage zone ($[?]29\Omega$, IQR: 28 - 33Ω) using similar levels of contact (**Figure 6**). Analysis of lesion depth by the number of splines with $CTC > 10\Omega$ revealed PEF treatment size was largely not impacted by catheter orientation or the number of splines in contact as long as stable CTC was achieved (**Figure 7**).

Discussion:

As new ablation modalities are introduced, it is important to develop tools that enable safe and effective treatment. For RF and Cryo, there have been decades of development to optimize the safety and efficacy of catheters, algorithms, and workflows. Innovations such as contact force sensing and real-time ablation indices have helped move thermal ablation workflows from empirical to reproducible¹¹. PEF ablation for arrhythmia treatment is still early in its development, as are the tools that will optimize its safe and effective

delivery. Most current PEF platforms rely on fluoro or ICE to guide ablation as EAM integration is limited. Overtreatment is commonplace, and tools confirming tissue contact are lacking.

This study sought to evaluate the utility of CTC for PEF ablation using a unique investigational LAF catheter, LI system, and PEF system. Ventricular lesions and atrial lesion sets were successfully created in ten swine with CTC assessed using LI. Treatment size, conduction block, and electrical isolation of target structures were examined acutely (N=8) and chronically (N=2) using EAM, pacing maneuvers, and tissue histology. No adverse events or collateral damage were observed. Analysis of LI, tissue characteristics, and EAM demonstrated that with a unique LAF catheter 1) CTC is critical for consistent and effective PEF treatment, 2) above a minimum contact threshold, increasing CTC does not increase treatment size, and 3) LI can be an effective tool for assessing CTC during PEF ablation, but its application will differ from that of focal RF.

Is Contact Needed for PEF Ablation?

Proximity of the field origin to targets and tissue homogeneity both directly influence the impact of a critical PEF voltage gradient⁷. Howard *et al*⁹ demonstrated *ex vivo* that maximum treatment size is achieved when a catheter is in apposition to target tissue while displacement of the electric field source from the tissue surface reduced lesion depth. Contact force and LI are both well-established indicators of CTC^{12,13}. In this study, with ICE guidance, LI consistently $>\Delta 10\Omega$ from baseline was found to be correlated to stable CTC. PEF treatments delivered with $>\Delta 10\Omega$ LI resulted in maximum treatment size and transmuralities while treatments delivered with $[\leq]\Delta 10\Omega$ LI (even with close proximity to tissue) resulted in reduced lesion size or no discernable lesion acutely and chronically. Intercaval lines containing 1-2 lesions with $[\leq]\Delta 10\Omega$ LI resulted in gaps. Therefore, the data indicate CTC can optimize PEF treatment similar to how thermal ablation feedback tools have improved workflows and patient outcomes¹⁴⁻¹⁶.

Does amount of contact matter for PEF ablation?

While research indicates a relationship between contact force and PEF treatment depth with focal catheters¹⁷, the LAF catheter investigated in this study did not demonstrate increased treatment depth with increased contact. LTC and HTC yielded similar lesion dimensions (approximately 6mm depth, 16mm width across all CTC ranges $>[\leq]10\Omega$). Unique catheter and electric field geometry contribute to this difference. Although LI is a measurement of electrode surface area in contact with resistive myocardium and not a direct measurement of contact force, LI has been shown to correlate with contact force over relevant operational ranges for focal catheters¹⁸. Similarly in this study, increased LI correlated with increased CTC; however, in contrast to a traditional solid-tip catheter, the LAF spheroid tip compresses in response to increased contact rather than indenting into the myocardium (**Supplemental Figure 1**). Additionally, solid-tip catheters produce small electric fields that are more susceptible to differences in contact than bigger LAF catheter electric fields⁷. These mechanical behaviors and field-size discrepancies may explain the differing impacts of increased contact force on PEF treatment sizes for compressible LAF catheters versus solid-tip catheters. This study also indicates that the number of splines in contact and the amount of each spline in contact with myocardium do not influence lesion size if the spline(s) have stable CTC (**Figure 7**).

With RF ablation, increased contact force leads to larger treatments, but also increased safety risks¹⁹. Increased CTC with the LAF catheter did not yield any additional safety risk. No damage to collateral structures, steam pops, perforations, or incidences of char were noted acutely or chronically for any CTC cohort. The spheroid catheter tip inherently lends itself to reduced risk of perforation and the flexibility of the nitinol splines allows force to be absorbed by the catheter rather than tissue, reducing tissue trauma. However, because the structure of the LAF catheter creates sizeable lesions even at LTC, splines that are in proximity to critical structures (e.g., AV node, HIS) should be closely monitored to prevent inadvertent damage. Tissue thinning and remodeling were noted after 30 days at ventricular lesion sites; observations similar to previous work with a different LAF catheter²⁰ and require further investigation (**Supplemental Figure 2**).

This study determines that, in relation to PEF treatment size and safety, the amount of CTC does not

matter once CTC is established with a LAF catheter. These results may extend to “single-shot” catheters where apposition to myocardium, rather than embedding a catheter tip into tissue, is the primary mode of operation²¹. It is critical to note that both catheter electrode configuration (e.g., electrode spacing, size) and system configuration (e.g., monopolar, bipolar) play important roles in contact dependence. Monopolar modalities have the ability to create deeper lesions for comparable energy outputs relative to bipolar configurations, making them more robust to intermittent contact⁷. Contact detection systems will need to be harmonized with PEF platforms to ensure appropriate feedback for the catheter design and delivery mechanism.

How should LI be used with PEF ablation?

Impedance metrics have been useful clinical tools in monitoring resistive heating and predicting lesion transmural depth for RF ablation^{22–24}. When used in a clinical RF workflow, targeting a >20 LI drop effectively predicted lesion efficacy and durability^{25,26}. For PEF ablation, LI is a useful way to measure CTC and confirm optimal catheter placement for lesion formation. However, LI may be limited in informing real-time PEF lesion formation. PEF ablation does not rely on electrode-tissue coupling to conduct current to tissue and cause resistive heating for cell death⁷. Therefore, starting impedance as an indicator of resistive potential or electrode coverage is not critical in PEF ablation. Once contact was established, no correlation was observed between starting impedance and treatment size in this study. Additionally, inconsequential impedance drops immediately post-PEF delivery (1-3) indicate negligible resistive heating is occurring from energy delivery (**Figure 6**). These PEF-specific differences limit the utility of impedance drop as an acute metric of therapy success. The effects of the induced electric field cause a cascade of cellular activity which impacts cell homeostasis and viability over the course of hours to days. LI, a wholistic measurement of tissue properties (e.g., temperature and relative health), changes with the evolution of myocardial damage and fibrosis²⁷. In previous RF studies, tissue impedance was reduced in more fibrotic tissue compared to healthy myocardium²⁸. Similarly, in this study, there was a substantial decrease in LI response on treated myocardium that presented evidence of transmural fibrosis at 30 days. When considering LI as an indicator of CTC, the decrease in feedback on scar tissue poses a potential shortcoming. Determining contact with previously treated myocardium or in fibrotic tissue will be challenging with LI and warrants further investigation.

Limitations:

This study was conducted in healthy swine and results may vary in humans or in scarred or diseased tissue. Lesion assessment was done on fresh TTC-stained tissue and all images were retrospectively analyzed for lesion dimensions using methods that are well established preclinically but impossible to validate clinically. Steps were taken to ensure measurement systems were calibrated correctly and TTC procedures were identical in all animals. All findings in this study use a proprietary biphasic waveform and investigational catheter design that may not be generally applicable for predicting treatment results of different PEF waveforms, systems, and catheters.

Conclusion:

This study confirmed the necessity and utility of CTC during monopolar PEF ablation of cardiac tissues via an investigational LAF catheter in a swine model. Using LI as an indicator, consistent CTC resulted in effective PEF ablation across a range of cardiac targets suggesting that contact, per se, is more important than the degree of contact. These results diverge from previous research using focal catheters, where increased contact resulted in increased lesion size and indicate LAF catheter require unique research and workflows. Lesion characteristics were optimized and reproducible across a wide range of LI changes and, notably, acute lesion characteristics were preserved chronically. These results suggest an important role for contact detection in the guided delivery of PEF energy.

Sources

1. Calkins H, Hindricks G, Cappato R, et al. 2017 HRS/EHRA/ECAS/APHRS/SOLAECE expert con-

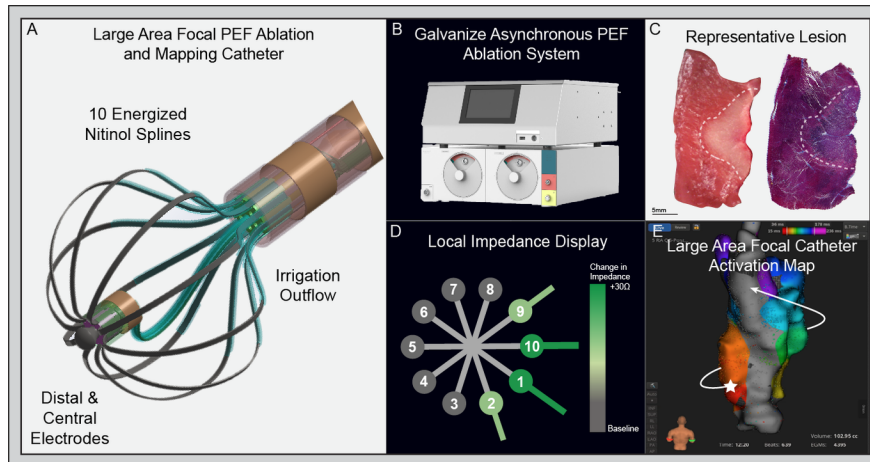
- sensus statement on catheter and surgical ablation of atrial fibrillation. *EP Europace* . 2018;20(1):e1-e160. doi:10.1093/europace/eux274
2. Natale A, Reddy VY, Monir G, et al. Paroxysmal AF catheter ablation with a contact force sensing catheter: results of the prospective, multicenter SMART-AF trial. *J Am Coll Cardiol* . 2014;64(7):647-656. doi:10.1016/j.jacc.2014.04.072
 3. Ikeda A, Nakagawa H, Lambert H, et al. Relationship Between Catheter Contact Force and Radiofrequency Lesion Size and Incidence of Steam Pop in the Beating Canine Heart: Electrogram Amplitude, Impedance, and Electrode Temperature Are Poor Predictors of Electrode-Tissue Contact Force and Lesion Size. *Circ: Arrhythmia and Electrophysiology* . 2014;7(6):1174-1180. doi:10.1161/CIRCEP.113.001094
 4. Su W, Kowal R, Kowalski M, et al. Best practice guide for cryoballoon ablation in atrial fibrillation: The compilation experience of more than 3000 procedures. *Heart Rhythm* . 2015;12(7):1658-1666. doi:10.1016/j.hrthm.2015.03.021
 5. Nuccitelli R. Application of Pulsed Electric Fields to Cancer Therapy. *Bioelectricity* . 2019;1(1):30-34. doi:10.1089/bioe.2018.0001
 6. Cabuy E, Miklavčič D, Nuccitelli R, Corp B. Pulsed Electric Fields in Cancer Treatment.
 7. Verma A, Asivatham SJ, Deneke T, Castellvi Q, Neal RE. Primer on Pulsed Electrical Field Ablation: Understanding the Benefits and Limitations. *Circ: Arrhythmia and Electrophysiology* . 2021;14(9). doi:10.1161/CIRCEP.121.010086
 8. Reddy VY, Koruth J, Jais P, et al. Ablation of Atrial Fibrillation With Pulsed Electric Fields. *JACC: Clinical Electrophysiology* . 2018;4(8):987-995. doi:10.1016/j.jacep.2018.04.005
 9. Howard B, Verma A, Tzou WS, et al. Effects of Electrode-Tissue Proximity on Cardiac Lesion Formation Using Pulsed Field Ablation. *Circ: Arrhythmia and Electrophysiology* . 2022;15(10). doi:10.1161/CIRCEP.122.011110
 10. Verma A, Neal R, Evans J, et al. Characteristics of pulsed electric field cardiac ablation porcine treatment zones with a focal catheter. *Cardiovasc electrophysiol* . 2023;34(1):99-107. doi:10.1111/jce.15734
 11. Szegedi N, Gellér L, Szegedi N, Gellér L. New Results in Catheter Ablation for Atrial Fibrillation. In: *Epidemiology and Treatment of Atrial Fibrillation* . IntechOpen; 2019. doi:10.5772/intechopen.88468
 12. Pesch E, Riesinger L, Vonderlin N, et al. Role of catheter location on local impedance measurements and clinical outcome with the new direct sense technology in cardiac ablation procedures. *IJC Heart & Vasculature* . 2022;42:101109. doi:10.1016/j.ijcha.2022.101109
 13. Kuck KH, Reddy VY, Schmidt B, et al. A novel radiofrequency ablation catheter using contact force sensing: Toccata study. *Heart Rhythm* . 2012;9(1):18-23. doi:10.1016/j.hrthm.2011.08.021
 14. Philips T, Taghji P, El Haddad M, et al. Improving procedural and one-year outcome after contact force-guided pulmonary vein isolation: the role of interlesion distance, ablation index, and contact force variability in the 'CLOSE'-protocol. *Europace* . 2018;20(FI.3):f419-f427. doi:10.1093/europace/eux376
 15. Berte B, Hilfiker G, Moccetti F, et al. Pulmonary vein isolation using ablation index vs. CLOSE protocol with a surround flow ablation catheter. *Europace* . 2020;22(1):84-89. doi:10.1093/europace/euz244
 16. Rottner L, Moser F, Weimann J, et al. Accuracy and Acute Efficacy of the Novel Injection-Based Occlusion Algorithm in Cryoballoon Pulmonary Vein Isolation Guided by Dielectric Imaging. *Circulation: Arrhythmia and Electrophysiology* . 2022;15(2):e010174. doi:10.1161/CIRCEP.121.010174
 17. Nakagawa H, Castellvi Q, Neal R, et al. B-PO03-131 EFFECTS OF CONTACT FORCE ON LESION SIZE DURING PULSED FIELD ABLATION. *Heart Rhythm* . 2021;18(8):S242-S243. doi:10.1016/j.hrthm.2021.06.605

18. Van Es R, Hauck J, Van Driel VJHM, et al. Novel method for electrode-tissue contact measurement with multi-electrode catheters. *EP Europace* . 2018;20(1):149-156. doi:10.1093/europace/euw388
19. Yokoyama K, Nakagawa H, Shah DC, et al. Novel contact force sensor incorporated in irrigated radio-frequency ablation catheter predicts lesion size and incidence of steam pop and thrombus. *Circ Arrhythm Electrophysiol* . 2008;1(5):354-362. doi:10.1161/CIRCEP.108.803650
20. Yavin HD, Higuchi K, Younis A, Anter E. Lattice-tip catheter for single-shot pulmonary vein isolation with pulsed field ablation. *J Interv Card Electrophysiol* . Published online November 28, 2022. doi:10.1007/s10840-022-01414-7
21. Groen MHA, van Driel VJHM, Neven K, et al. Multielectrode Contact Measurement Can Improve Long-Term Outcome of Pulmonary Vein Isolation Using Circular Single-Pulse Electroporation Ablation. *Circulation: Arrhythmia and Electrophysiology* . 2022;15(8):e010835. doi:10.1161/CIRCEP.121.010835
22. Das M, Luik A, Shepherd E, et al. Local catheter impedance drop during pulmonary vein isolation predicts acute conduction block in patients with paroxysmal atrial fibrillation: initial results of the LOCALIZE clinical trial. *EP Europace* . 2021;23(7):1042-1051. doi:10.1093/europace/euab004
23. García BI, Ramos P, Luik A, et al. Local Impedance Drop Predicts Durable Conduction Block in Patients With Paroxysmal Atrial Fibrillation. *JACC: Clinical Electrophysiology* . 2022;8(5):595-604. doi:10.1016/j.jacep.2022.01.009
24. Solimene F, Giannotti Santoro M, De Simone A, et al. Pulmonary vein isolation in atrial fibrillation patients guided by a novel local impedance algorithm: 1-year outcome from the CHARISMA study. *Journal of Cardiovascular Electrophysiology* . 2021;32(6):1540-1548. doi:10.1111/jce.15041
25. Fukaya H, Mori H, Oikawa J, et al. Optimal local impedance parameters for successful pulmonary vein isolation in patients with atrial fibrillation. *J Cardiovasc Electrophysiol* . 2023;34(1):71-81. doi:10.1111/jce.15748
26. Solimene F, Schillaci V, Stabile G, et al. Prospective evaluation of local impedance drop to guide left atrial posterior wall ablation with high power. *J Interv Card Electrophysiol* . 2022;65(3):675-684. doi:10.1007/s10840-022-01317-7
27. Amorós-Figueras G, Jorge E, García-Sánchez T, Bragós R, Rosell-Ferrer J, Cinca J. Recognition of Fibrotic Infarct Density by the Pattern of Local Systolic-Diastolic Myocardial Electrical Impedance. *Front Physiol* . 2016;7:389. doi:10.3389/fphys.2016.00389
28. Myocardial electrical impedance mapping of ischemic sheep hearts and healing aneurysms. doi:10.1161/01.CIR.87.1.199

	No Contact Cohort	Low Contact Cohort	High Contact Cohort
Average # Ablations per Intercaval	18 ± 4	22 ± 3	19 ± 5
Average Pre-Ablation Impedance (Ω)	NTC Lesions: 10 ± 4 HTC Lesions: 35 ± 8	22 ± 6	38 ± 8
Intercaval Block	Acute (n=3): 0% Chronic: N/A	Acute (n=4): 100% Chronic (n=1): 100%	Acute (n=3): 100% Chronic (n=1): 100%
Total Intercaval Ablation Time (mins)	2.44 ± 0.89	2.87 ± 0.73	2.59 ± 1.09
Average # of Ablations per PVI	-- †	15 ± 5	15 ± 2
Average Pre-Ablation Impedance (Ω)	-- †	23 ± 9	32 ± 6
PV Isolation	-- †	Acute (n=4): 100% Chronic (n=1): 100%	Acute (n=4): 100% Chronic (n=1): 100%
Total PVI Ablation Time (mins)	-- †	2.00 ± 0.28	1.97 ± 0.59
†NTC intercaval line (HTC lesions interposed with 1-2 NTC lesions) workflow was only completed in the RA in acute subjects			

Table 1. Atrial Lesion Set Data by Catheter-Tissue Contact Cohort

Figure 1. LAF Catheter with Investigational PEF Ablation and LI Measurement Systems



A. LAF catheter featuring 10 splines for energy delivery and 4 additional electrodes for sensing and tracking. **B.** Investigational PEF system: generator and connection box. **C.** Representative lesion with a single application of 25A PEF energy (**C Left** : TTC stained lesion, **C Right** : Fixed lesion with Masson's trichrome staining). **D.** LI graphical user interface (GUI) featuring an *en face* representation of the LAF catheter tip. **E.** EAM post ablation map using the LAF catheter.

Figure 2. Pre-Defined Catheter-Tissue Contact Cohorts: **A.** NTC Example: ICE image of the LAF catheter (outlined in white) in close proximity to the tissue surface (dotted yellow). No color change in LI GUI as impedance change is < 10 threshold. **B.** LTC Example: ICE image of catheter touching the tissue surface and light green GUI tip graphic corresponding to light contact. **C.** HTC Example: ICE shows some deformation of the spheroid tip while pushing into tissue and dark green GUI tip graphic corresponding to heavy contact. All lesions were assigned to one of the three CTC cohorts prior to energy delivery.

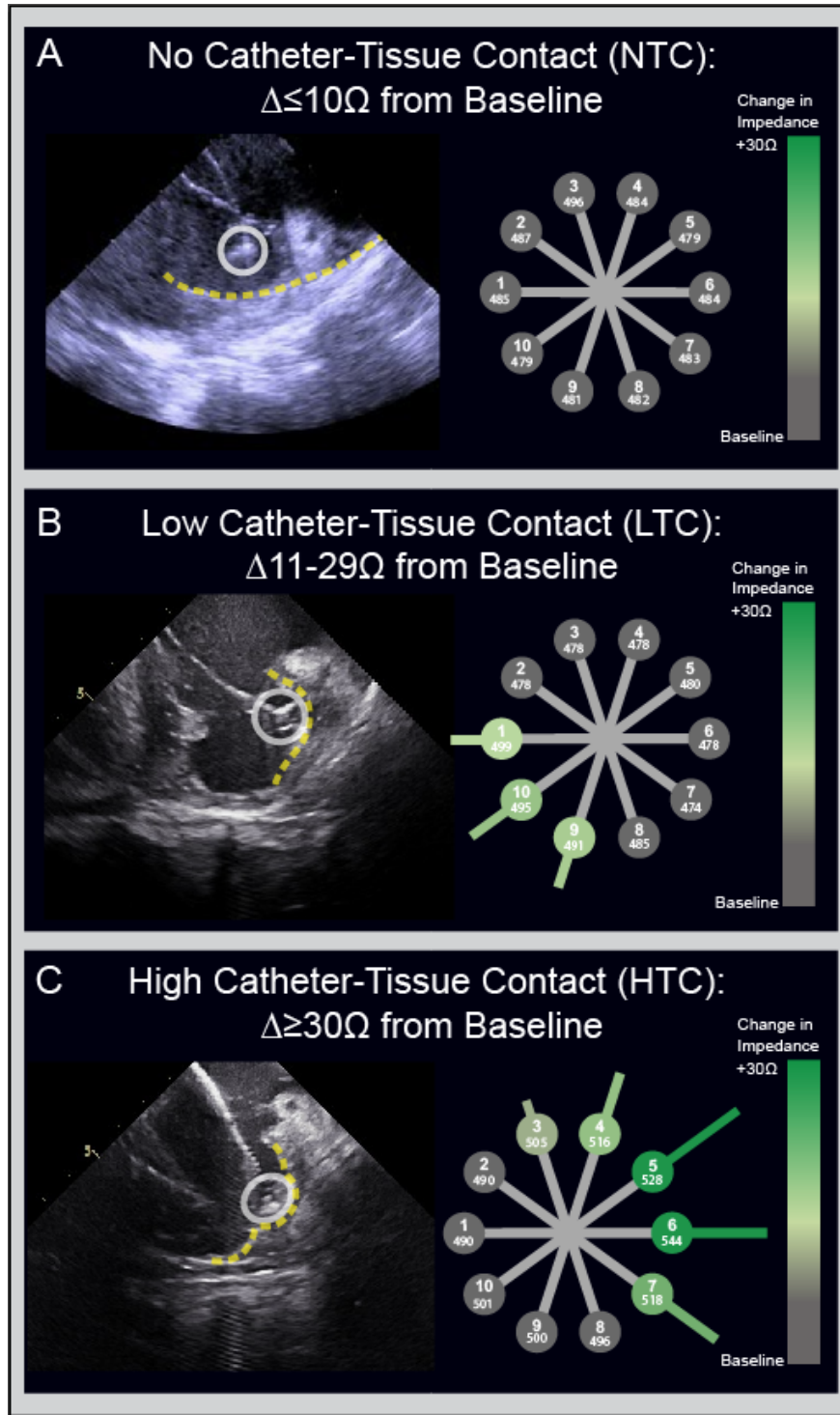


Figure 3: Acute Ventricular Lesion Data **A.** Pre-ablation LI deltas from all lesions. **B.** Representative TTC-stained lesions for each CTC cohort. **C.** NTC lesions are statistically smaller than LTC and HTC lesions. Lesion dimensions do not continue to increase once LI > 10 is achieved.

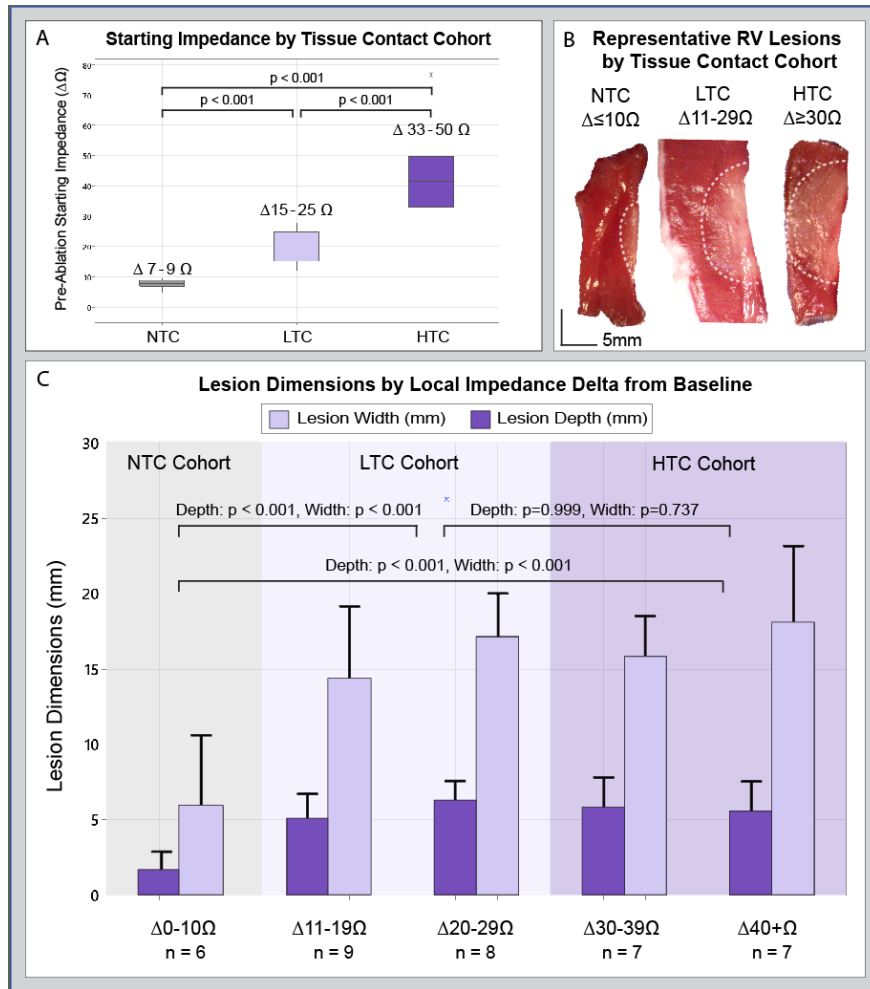
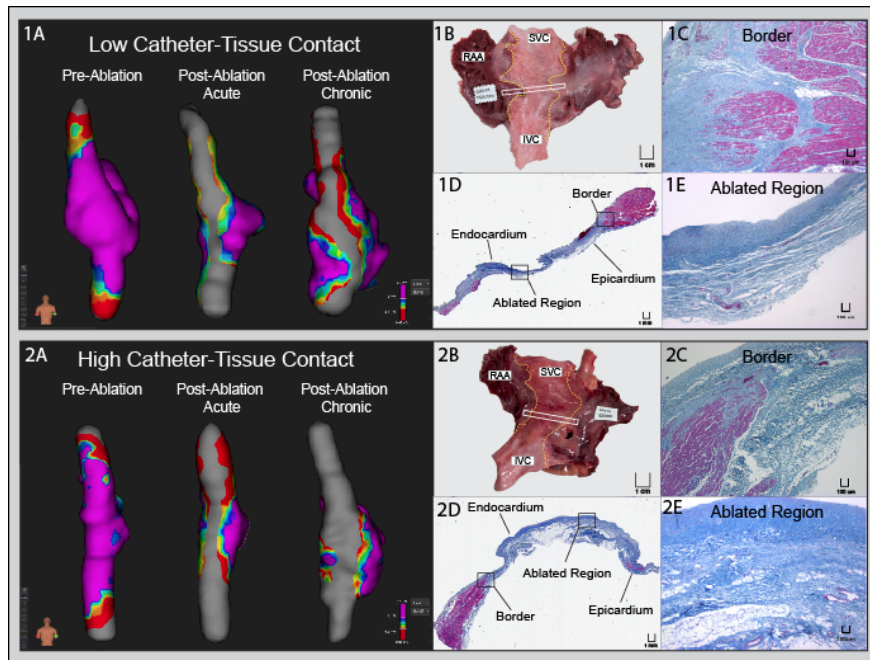


Figure 4. Representative electroanatomic maps and histology



1A and 2A. Pre-Ablation, acute, and chronic voltage maps (0.1-1mV) of RA intercaval lines treated with LTC and HTC. **1B and 2B.** Gross pathology of representative intercaval lines (outlined in dotted yellow) show areas of damage and samples of this tissue (white boxes) with Masson's Trichrome stain demonstrate pink, healthy myocardium on unablated border regions (**1C,D and 2C,D**), and transmurular blue fibrosis for both LTC and HTC lesions (**1E and 2E**).

Figure 5: NTC Intercaval Line A. EAM of an NTC intercaval line shows low voltage where HTC lesions were placed and high voltage where the NTC lesion was placed. Tissue treated with NTC also showed no signs of significant damage in gross pathology (**C**), or in histology with Masson's Trichrome staining (**D**) while areas treated with HTC showed gross damage (**C**, yellow dotted line) and signs of edema and myocytolysis in histology (**B**).

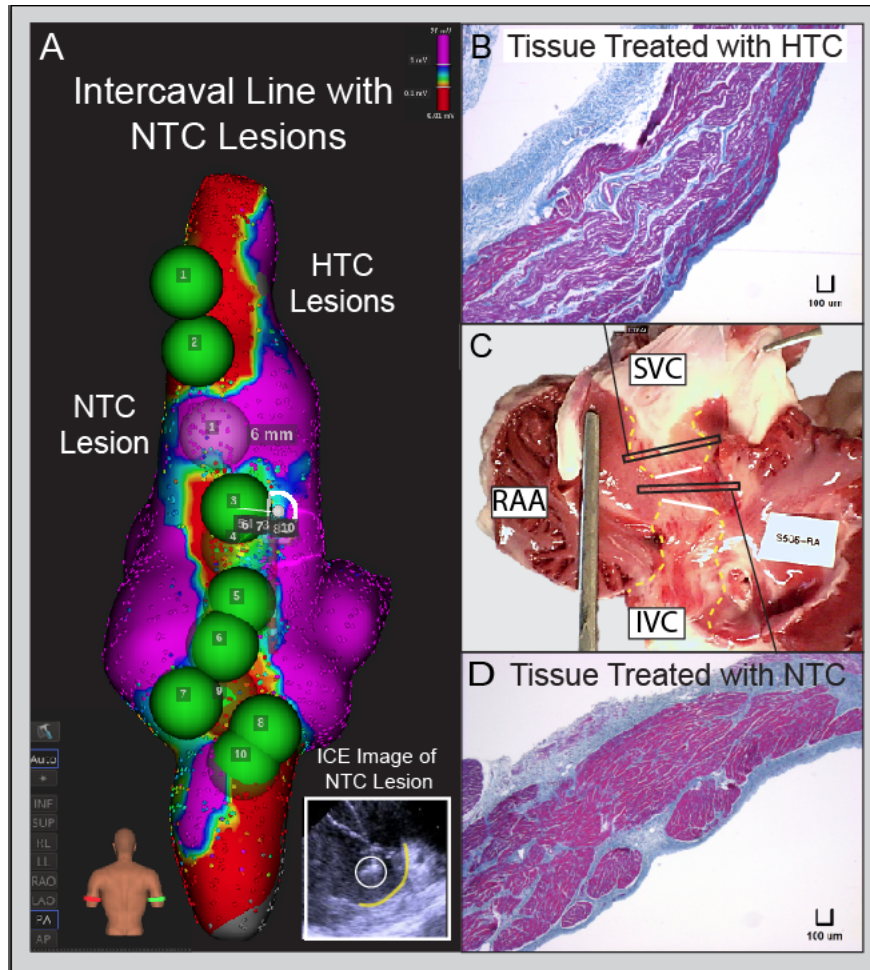


Figure 6: LI Drop & LI on Treated Tissue **A.** Comparison of pre-ablation and post-ablation local impedance by CTC cohort. **B.** LI response at 30 days by bipolar electrogram voltage.

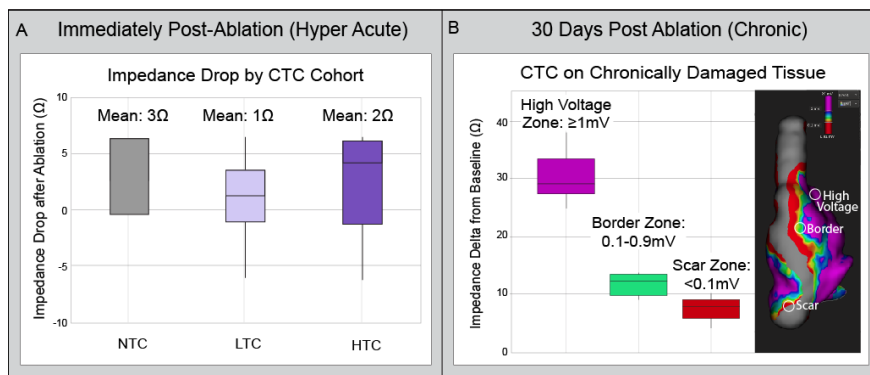
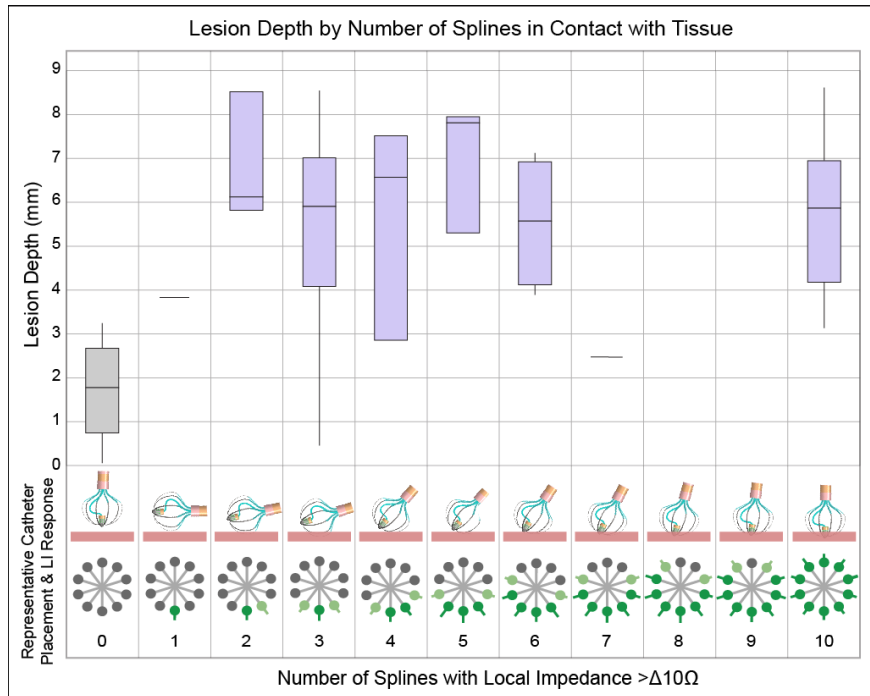
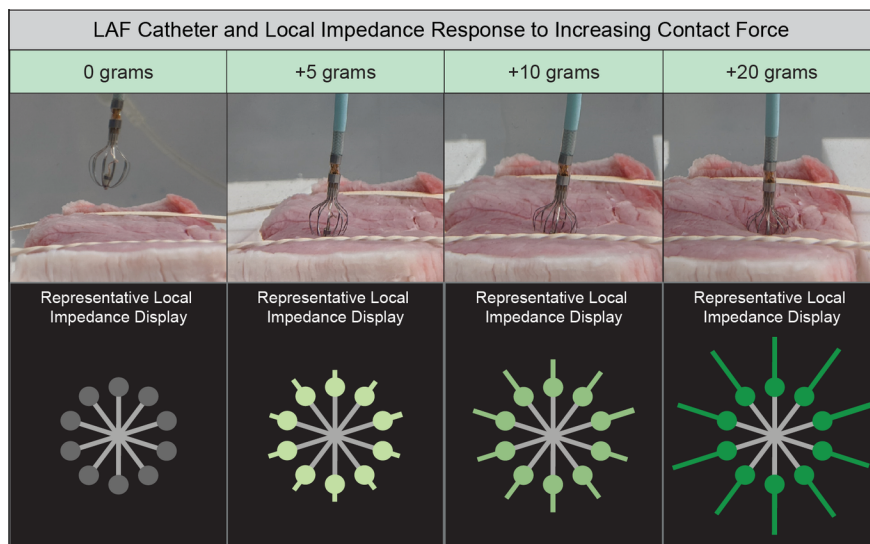


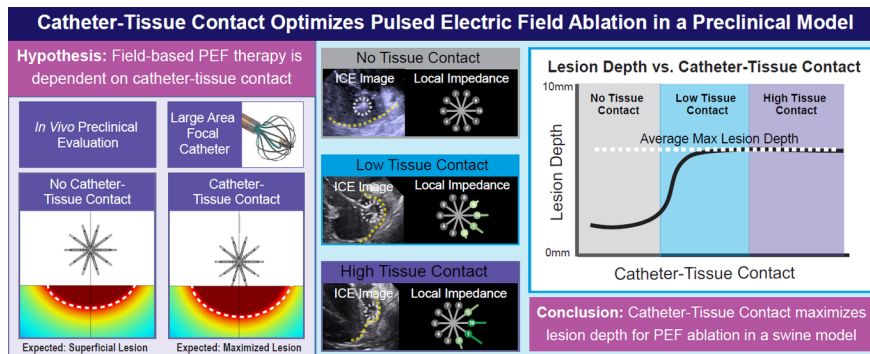
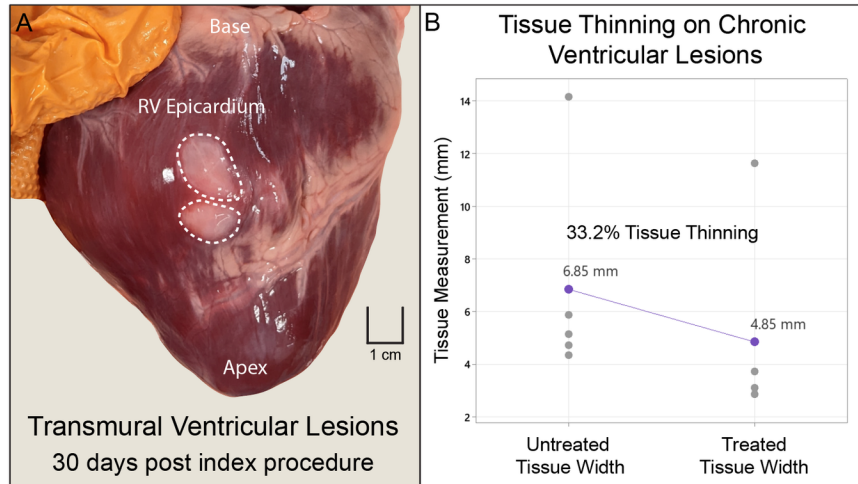
Figure 7. Number of Splines in Contact: Catheter orientation can be estimated by evaluating the number of splines showing $>[?]10$ LI from baseline. Once a minimum of 2 splines have consistent CTC $>[?]10$, lesion depth does not change substantially.



Supplemental Figure 1: Increased contact causes distortion of both the tissue and the LAF catheter. The LI display can be calibrated to show a proportional response to increased contact.



Supplemental Figure 2: **A.** RV lesions are visible from the epicardium after 30 days, showing transmural and significant remodeling. **B.** Fibrosis of treated RV wall tissue resulted in roughly 33% thinning of the ventricular wall.



Graphical Abstract